



Materials and Energy Research Center

MERC

Contents lists available at [ACERP](#)

Advanced Ceramics Progress

Journal Homepage: www.acerp.ir

Advanced Ceramics Progress

Original Research Article

Comparative Study of Anodized Titanium Surfaces: The Effect of Low Voltage on the Morphology, Performance, and Corrosion Resistance of the Double Layer

Ali Shanaghi ^{a,*}, Ali Reza Souri ^{b,*}, Wrya Forghani ^c^a Associate Professor, Department of Materials Engineering, Faculty of Engineering, Malayer University, Malayer, Iran, P.O. Box 65719-95863^b Assistant Professor, Department of Materials Engineering, Faculty of Engineering, Malayer University, Malayer, Iran, P.O. Box 65719-95863^c MSc, Department of Materials Engineering, Faculty of Engineering, Malayer University, Malayer, Iran, P.O. Box 65719-95863* Corresponding Authors' Emails: a.shanaghi@malayeru.ac.ir (A. Shanaghi); arsouri@gmail.com (A. R. Souri)URL: https://www.acerp.ir/article_169260.html

ARTICLE INFO

ABSTRACT

Article History:

Received 31 January 2023
 Received in revised form 27 February 2023
 Accepted 5 April 2023

Keywords:

Anodizing
 Low Voltage
 Ti Alloy
 Simulated Body Fluid Solution
 Corrosion Behavior
 Double Layer

The anodizing process of titanium (Ti) implants and their alloys improves their corrosion resistance and life service by naturally increasing the thickness of the passive oxide layer formed on the surface. Among the parameters that affect the properties of the anodized layer, voltage is a significant one due to the kinetic and thermodynamic processes. In this paper, commercial pure titanium (cp-Ti) coupons with the dimensions of $20 \times 10 \times 1 \text{ mm}^3$ were used as the anode in 1 M sulfuric acid solution at different voltages of 3, 6, and 9 V, current intensity of 3 A, electrolyte temperature of 60 °C, and duration time of 30 s. The phase composition analysis, morphology, and corrosion behavior of the anodized Ti were examined by Grazing-Incidence X-Ray Diffraction (GIXRD), Field-Emission Scanning Electron Microscopy (FESEM), and electrochemical impedance, respectively, in Simulated Body Fluid (SBF) at 37 °C. The results confirmed the formation of titanium oxide coating with a hexagonal structure. A smoother surface was obtained upon increasing the voltage up to 6 V. However, the surface became rougher with further voltage increase up to 9 V. The highest charge transfer resistance (37354 and 58127 ohm.cm^{-2}) was achieved at 6 V after 1 and 24 hours of immersion in the SBF solution, representing 84 % and 2440 % increase, respectively, compared to the cp-Ti sample. The double layer helps prevent the formation of localized corrosion sites, such as pitting and crevice corrosion, which can be particularly damaging to Ti alloy as an implant in the human body. Although rising the voltage from 3 to 6 V resulted in a more hydrophobic surface (as shown by an increase in the contact angle from 63.8° to 74.1°), further voltage increase up to 9 V made the surface more hydrophilic than before.


<https://doi.org/10.30501/acp.2023.383589.1116>

1. INTRODUCTION

Affected by rapid improvement in the living standards and progress in the societies in general, human beings have been more exposed to social pressures imposed by the spread of different types of diseases limiting human

life expectancy. Microsurgery and use of biological materials like antibacterial agents and antibiotics are some of the most effective ways to preserve and extend human lives [1]. Despite its benefits, it can also be costly due to the financial burden it puts on the patient's insurance services [2]. Biological materials, however,

Please cite this article as: Shanaghi, A., Souri, A. R., Forghani, W., "Comparative Study of Anodized Titanium Surfaces: The Effect of Low Voltage on the Morphology, Performance, and Corrosion Resistance of the Double Layer", *Advanced Ceramics Progress*, Vol. 9, No. 2, (2023), 1-7. <https://doi.org/10.30501/acp.2023.383589.1116>

2423-7485/© 2023 The Author(s). Published by MERC.

This is an open access article under the CC BY license (<https://creativecommons.org/licenses/by/4.0/>).

can cause mechanical failure, infection, and reactions in relation to racial immunity. In this regard, there have been considerable research efforts to improve these materials in order to continue physiological processes and vital functions for survival [3]. One of the most popular metal materials for medical applications is titanium alloys. Ti-6Al-4V has been widely used in biomedical applications for a long time. However, it has been found to have potential toxic effects caused by the release of vanadium and aluminum ions [4]. This has encouraged the researchers to focus on commercial pure titanium (cp-Ti), the best biocompatible metallic material owing to its surface properties that spontaneously produce a neutral and stable oxide layer. Several of its characteristics such as low electron conductivity, stable thermodynamic state at the body pH values, and low tendency to take form in aqueous media make it an ideal choice for medical applications [4]. Additionally, its surface can be further enhanced through anodizing processes that results in the formation of a thicker, more corrosion-resistant layer. Therefore, titanium is a preferable choice for medical implants due to its better biocompatibility and strength [5-7].

Anodizing is one of the surface improvement processes that can lead to the formation of a thick oxide layer on a metal substrate. Aluminium, Titanium, Tantalum, Niobium, Vanadium, Hafnium, and Tungsten are known as the valve metals since they are quickly covered with a thin homogenous oxide layer when exposed to oxygen-rich environments [8-9]. This protective oxide layer helps slow down the reaction rate on the metal surface; therefore, these metals are widely used to protect metals from corrosion [9-10].

Despite extensive studies on the strength and biocompatibility of titanium implants, few studies have been conducted to compare the growth of the anodic oxide on the valve metal surfaces [11-12]. The thickness of the titanium oxide layer depends on the electrolyte solution, pH value, applied voltage, current density, and anodizing time. As a result, these factors can lead to the formation of thicker and porous oxide layers among which, voltage is more remarkable than the other environmental ones since the valence state of the cations within the passive film is highly dependent on the passive potential. This valence state can then affect the doping density, flat band potential and ultimately, corrosion protection [13]. Moreover, the composition and structure of the passive film will determine the corrosion protection, and different compounds and structures can cause different protective effects. In the anodizing process, different electrolytes, sulfuric acid [14-16], phosphoric acid [17-18], and oxalic acid [19-21] are used. In general, sulfuric acid is the most commonly used electrolyte solution due to its lower price and high rate of oxide layer formation [14-16].

Anil Kumar found that the anodic current density increased upon increasing the applied voltage and

temperature of the electrolyte, and the incremental change in the anodizing voltage leads to changes in the deposition rate of the oxide layer as well as the pore diameter [22], color of the oxide layers, slope between the applied current density, and anodization time. However, they did not report the relation between the porous properties of titanium oxide and voltage of the anodizing process. In this regard, we conducted a systematic study of the anodization conditions of cp-Ti substrate in 1 M sulfuric acid solution at different low voltages and then investigated the phase, structural and morphological properties as well as the corrosion behavior of the samples through electrochemical tests and electrochemical impedance in Simulated Body Fluid (SBF) at 37 °C.

2. MATERIALS AND METHODS

The commercial Ti foils (Ti, 99.33 %) with elemental analyses (Table 1) were annealed according to ASTM B265-10 and cut into 20×10 mm² pieces that were 2 mm thick. The pieces were then polished with sandpaper ranging in grit from 800 to 3,000 and alumina slurry solution of 0.5 μm in diameter. After polishing, the samples were degreased and ultrasonically rinsed for 10 min in acetone (99.5 %, Merck), ethanol (97 %, Merck), and deionized water. The cleaned Ti specimens were then electropolished in a mixture of hydrofluoric acid (HF, 40 %, Merck) and nitric acid (HNO₃, 65 %, Merck) (volume ratio = 1:8) for 90-120 s and rinsed with deionized water and dried in air. All chemicals were used as received without further purification.

The anodizing process [11,14-16] was then conducted in an electrochemical two electrode cell containing 200 ml 1 M sulfuric acid (H₂SO₄, 95-97 %, Merck) solution at 60 °C for 30 seconds with three different low voltages (3, 6, and 9 V) at the constant current of 3 A.

The phase, structure, and morphology of the coatings were determined using Grazing- Incidence X- Ray Diffraction (GIXRD; Philips PW- 1730 X- ray diffractometer; Cu Kα, λ = 0.154056 nm) and Field-Emission Scanning Electron Microscopy (FE-SEM; MIRA3 TESCAN). The thickness of the coatings was determined by the FE-SEM cross section. The water contact angles were measured on the contact angle goniometer (model 200-00-115, Ramé-Hart Instrument Co.), and the surface energy was calculated by the DROP image standard software (harmonic mode) and Owens-Wendt method [23-24].

The corrosion test was done in a the SBF solution containing 7.996 g of NaCl, 0.35 g of NaHCO₃, 0.224 g of KCl, 0.228 g of K₂HPO₄.3H₂O, 0.305 g of MgCl₂.6H₂O, 40 mL of 1 M HCl, 0.278 g of CaCl₂, 0.071 g of Na₂SO₄, and 6.057 g of (CH₂OH)₃CNH₂ at 37 °C while the pH was adjusted at 7.25 with 1 M HCl. Electrochemical Impedance Spectroscopy (EIS) and

potentiodynamic polarization tests were carried out on the electrochemical workstation (IviumSTAT, Netherlands). The corrosion characteristics were evaluated in a cell composed of the anodized sample as a working, Ag/AgCl as a reference, and platinum mesh as an auxiliary electrode in 250 ml SBF. The surface area was about 1 cm². The EIS was performed from 10⁻¹ to 10⁵ Hz by applying 10 mV as the amplitude and frequency of 20 mHz in the sweeping mode. To investigate the corrosion mechanism of the coatings, the impedance tests were done at 1 and 24 h, and the corroded surfaces of the anodized samples after 24 h were investigated by the FE-SEM image.

TABLE 1. The Elemental analysis of cp-Ti determined by optical emission spectrometer

Element	Ti	C	N	H	O	Fe
(wt. %)	99.33	0.08	0.03	0.01	0.25	0.30

3. RESULTS AND DISCUSSION

The anodizing process improves the microstructural properties, shape, and corrosion resistance of titanium oxide by thickening the natural titanium oxide layer on its surface. The anodizing voltage of the process has a huge impact on the oxidation reaction in terms of speed, shape, and microstructure of titanium oxide. In this paper, the anodizing process was carried out using 3, 6, and 9 volts on the cp-Ti substrate.

Figure 1 shows the GIXRD curve of the anodized sample. According to the standard card Titanium oxide, the main peaks at different angles from the anatase TiO₂ (JCPDS 01-072-1807) are 39.39°, 37.93°, and 34.95° related to the crystal plates (-1-12), (004), and (110), respectively, and the 53.01°, 63°, 70.7°, and 76.2° related to the (222), (213), (322), and (231), respectively, appeared from the Ti substrate (JCPDS 21-1272). These peaks are indicative of the hexagonal crystal structure of titanium oxide [6,11].

Upon increasing the voltage from 3 volts to 9 volts, the FE-SEM images of the anodized titanium samples at 3, 6, and 9 (Figure 2) show an improvement in the uniformity and homogeneity of the anodized cp-Ti. However, according to the literature [9,11,22], increasing the anodizing voltage at a high value would increase the deposition rate of the oxide layer or thickness as well as the pore diameter.

The surface wettability, which is related to the surface energy of a body, is one of the surface characteristics that affects its biological capabilities. Generally, hydrophilic surfaces improve the adhesion, proliferation, cell division, and bone mineralization [11,22]. The results of water contact angle measurements are summarized in Table 2. as observed, the lower the water contact angle, the higher the wettability.

According to the literature, hydrophilicity increased by increasing the surface roughness; however, the surface could become either superhydrophilic or superhydrophobic when it was very smooth. The obtained

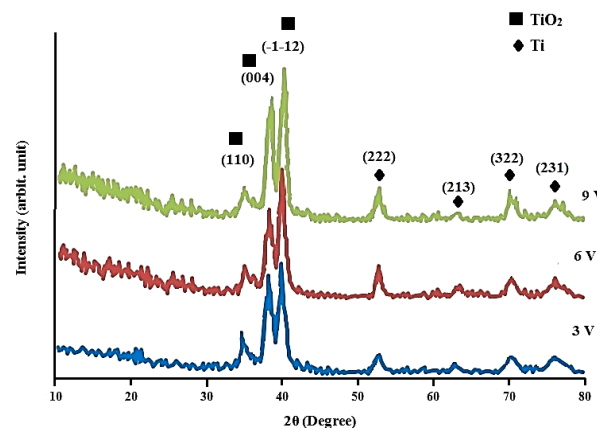
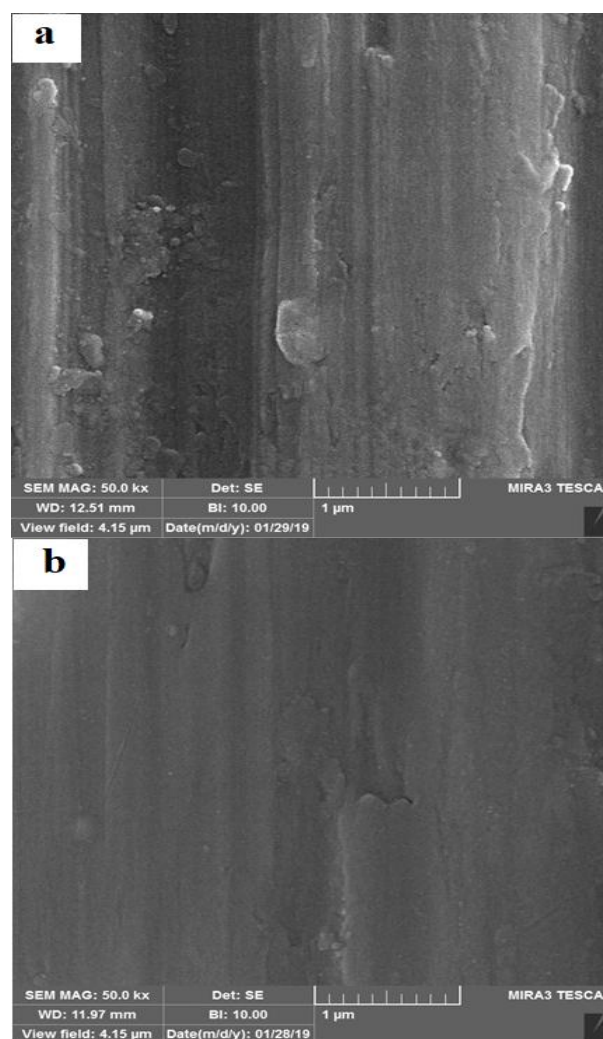


Figure 1. GIXRD curve of anodized titanium sample at low voltages such as 3, 6, and 9 volts at an incidence angle 1°



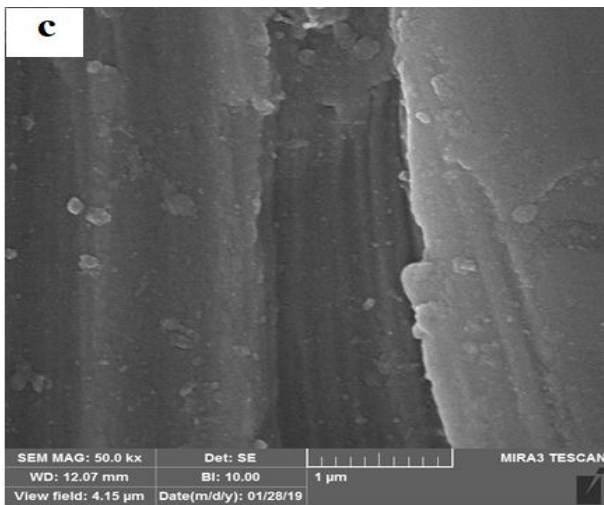


Figure 2. FE-SEM image of anodized titanium at different low voltages, a) 3 volts, b) 6 volts, and c) 9 volts

TABLE 2. Water contact angle of cp- Ti substrate and anodized cp-Ti at low voltages 3, 6, and 9 V

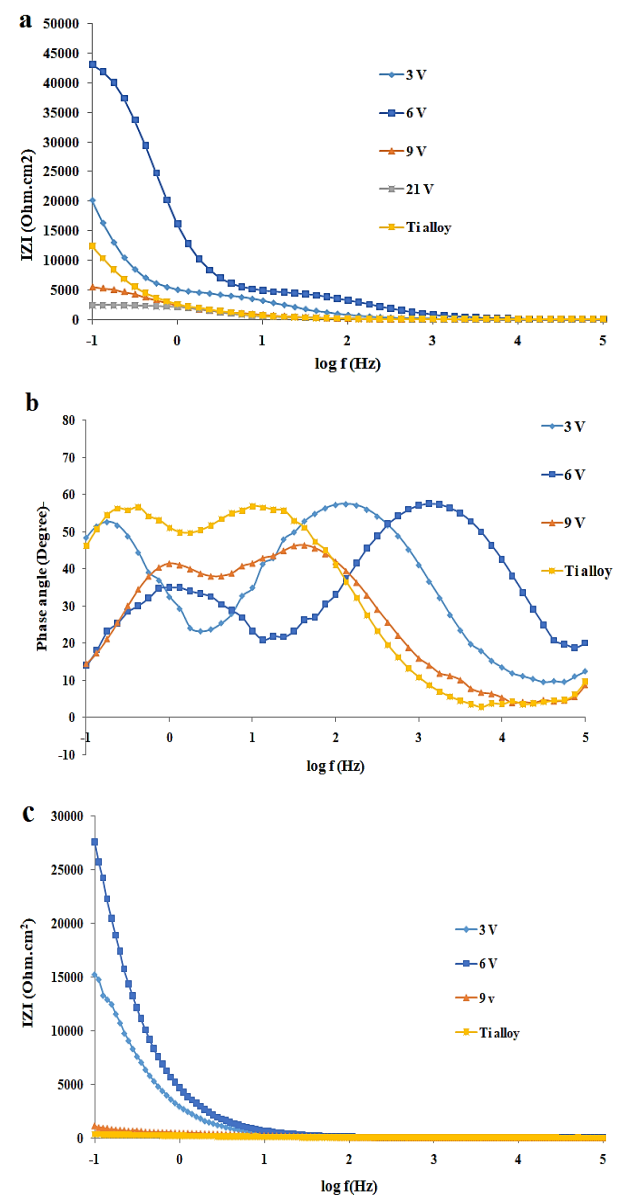
Specimen	Contact angle (Degree)
cp-Ti	103.7
Anodized cp-Ti at 3 V	63.8
Anodized cp-Ti at 6 V	74.1
Anodized cp-Ti at 9 V	57.2

results showed that anodizing the titanium substrate would increase its hydrophilicity by creating titanium oxide on the surface and increasing its surface roughness (confirmed by FE-SEM images in Figure 2). Increasing the voltage from 3 to 6 volts increased the contact angle from 63.8° to 74.1°, thus making the surface more hydrophobic. However, increasing the voltage from 6 to 9 volts increased the hydrophilicity of the surface, and water droplets spread rapidly on the surface under the capillary effect [11,25].

According to the bode and bode-phase plots, applying the anodizing voltage of 6 V resulted in a more capacitive behavior at higher frequencies than that at other voltages, and the diffusion of water from surface defects of anodized cp-Ti sample at 3 and 9 V caused resistance behavior at a high frequency. In addition, the presence of two-time constants in the bode-phase curve is indicative of the presence of oxide layers and obstacles in the path of electrons between the SBF solution and titanium substrate as well as the formation of a double layer at their interface. However, upon increasing the immersion time (Figure 3a), As a result of the penetration of water ions into the anodizing oxide layer and presence of soluble ions on the layer, especially for 6 V sample, a decrease in the corrosion resistance was observed with a reduction in the phase angle at high frequencies. The existence of a wide time constant for 3 and 6 V confirms the formation of homogeneous and uniform corrosion

products on the anodized cp-Ti sample at 24 h in the SBF solution compared to other samples (Figure 3c). This corrosion behavior at low voltages can be attributed to the formation of the corrosion products on the anodized surface, compared to the non-anodized sample [6-7], as well as the homogeneity, uniformity, and defect-free corrosion of the products on the surface of the anodized samples at low voltages of 3 and 6 V, all more than those at 9 V.

In order to accurately evaluate the corrosion behavior, electrochemical systems were simulated as an electrical circuit containing a resistor and a capacitor. This circuit is related to the capacity of the dual layer which has two plates with an arrangement of opposite charges, and the resistance of this layer is referred to as the dual layer resistance or charge transfer resistance. Double layer



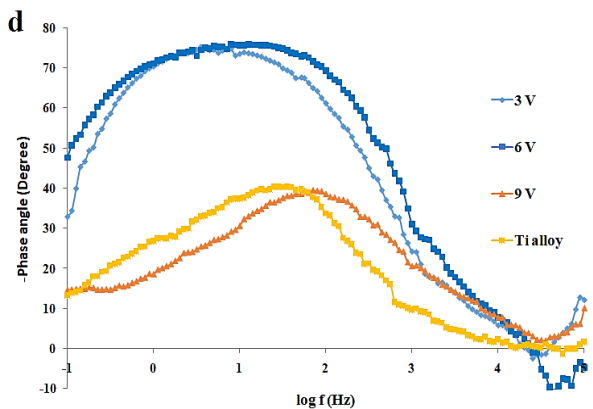


Figure 3. Bode and bode-phase plots of cp-Ti alloy, and anodized cp-Ti at low voltage, 3 V, 6 V, and 9 V, at two immersion times a-b) 1 h and c-d) 24 h

refers to the electrochemical structure that develops at the interface between a metal surface and an electrolyte solution. The double layer consists of two layers of charge, known as the Helmholtz and diffuse layers. The Helmholtz layer is a compact layer of adsorbed ions and water molecules that are directly attached to the metal surface while the diffuse layer is a less ordered layer of ions that surround the Helmholtz layer. The performance of the double layer on the corrosion behavior of anodized titanium is an important factor to consider. The double layer formed at the interface between the anodized titanium surface and electrolyte plays a crucial role in the corrosion behavior of the material. The protective oxide layer formed during anodization acts as a barrier to limit the access of the corrosive species to the underlying metal surface while the double layer helps repel the charged species that could cause corrosion [6-7]. The proposed equivalent circuit is demonstrated in Figure 4 for the cp-Ti and anodized cp-Ti at low voltages of 3, 6, and 9 volts, and the results are shown in Table 3. R_{ct} is associated with the charge transfer resistance of the dual layer, and CPE_{dl} to the dual layer capacitance.

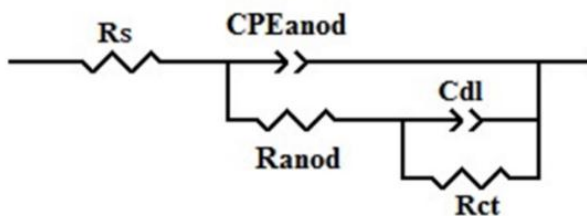


Figure 4. Equivalent circuit of cp-Ti substrate and anodized cp-Ti specimens at low voltages of 3, 6, and 9 volts

The charge transfer resistance (R_{ct} ; $\Omega \cdot \text{cm}^2$) and n of the cp-Ti substrate and anodized cp-Ti specimen at 3, 6, and 9 volts after an hour in the SBF solution (Table 3) show

the higher resistance along with the enhanced homogeneity and uniformity of the coating surface while increasing n for the anodized cp-Ti specimens at 6 V, compared to the other voltages. Generally, anodizing causes an increase in the heterogeneity and roughness, which was clear for the anodized samples at 3 and 9 V, thus leading to a decrease in the corrosion resistance due to the increased surface imperfections and intensity of the local corrosion reactions, compared to 6 V. Results of Table 3 denoted that prolonging the immersion time from 1 to 24 hours intensifies the corrosion reactions and enhances the charge transfer resistance between the SBF solution and sample surface. In fact, the anodization process results in the formation of a porous oxide layer on the titanium surface, which increases the surface area and facilitates the formation of a more robust double layer. The thickness and properties of the oxide layer can be controlled by adjusting the anodization parameters such as the voltage, current density, and electrolyte composition. Studies have shown that compared to the non-anodized titanium surface, the anodized titanium surface with a well-formed double layer exhibited significantly improved corrosion resistance.

TABLE 3. Parameters obtained from the equivalent circuit of cp-Ti substrate and anodized cp-Ti specimens at low voltages of 3, 6, and 9 volts

Time period (h)	Sample	CPE_{dl} ($\mu\text{F} \cdot \text{cm}^{-2} \cdot \text{s}^{-n}$)	R_{ct} ($\Omega \cdot \text{cm}^2$)	n_{dl}	Chi-squared
1	Ti alloy	59.91	20235	0	0.00189
	TiA3	71.17	36179	0	0.00335
	TiA6	9.839	37354	0	0.01135
	TiA9	69.28	4127	0	0.00142
24	Ti alloy	2523.27	2287	0.65	0.00195
	TiA3	24.79	20995	0.86	0.00454
	TiA6	34.62	58127	0.81	0.00668
	TiA9	1586.42	6391	0.85	0.00546

In summary, the significant increase in the surface heterogeneity (n) of the cp-Ti sample and anodized cp-Ti samples at low voltage of 6 V, compared to 3 and 9 V, after 24 hours that was confirmed by FE-SEM images (Figure 5) obtained from the EIS study at 24 hours in the SBF solution. The double layer helps prevent the formation of localized corrosion sites such as pitting and crevice corrosion, which can be particularly damaging to titanium. Overall, the performance of the double layer and its effect on the corrosion behavior of the anodized titanium is of significance while maintaining the material's corrosion resistance properties. The anodization process can be used to form a protective oxide layer on the titanium surface, which enhances the double layer and improves the corrosion resistance of the material [6-7,9-10].

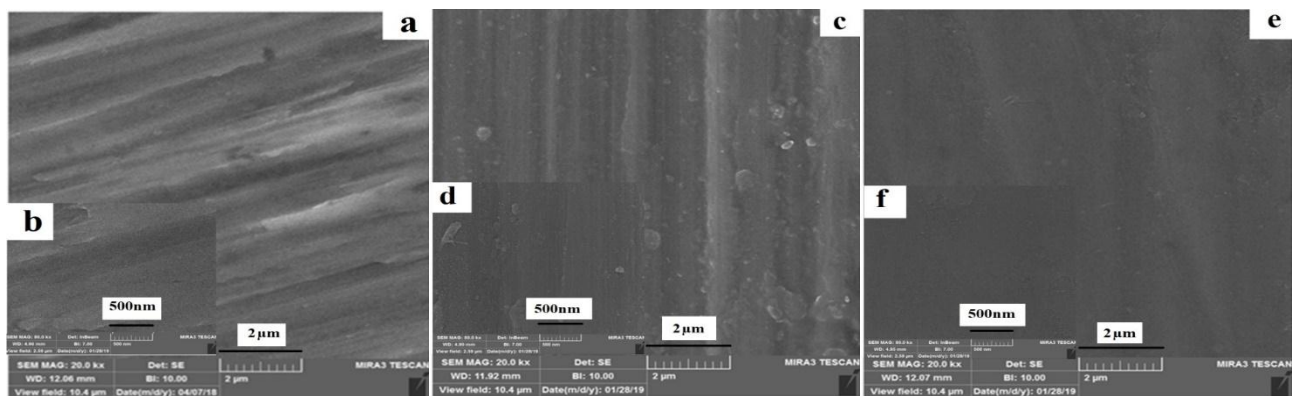


Figure 5. FE-SEM images of anodized cp-Ti at low voltage, a-b) 3 V, c-d) 6 V, and e-f) 9 V after 24 h of immersion in SBF solution

4. CONCLUSION

The studies on the effect of low anodizing voltage on the corrosion behavior of cp-Ti specimens revealed that 6 volts could be an optimal voltage for titanium oxide formation with hexagonal structure that also ensured higher corrosion resistance than that of other anodized samples at 3 and 9 volts. Upon further increasing the voltage above 6 volts, both surface imperfections and roughness were enhanced that led to the intensity of local reactions due to the penetration of water and corrosive ions, thus resulting in the reduced corrosion resistance of the anodized sample at 9 V. Of note, the double layer prevented the formation of localized corrosion sites, such as pitting and crevice corrosion, which can be particularly damaging to titanium alloy as an implant in the human body. Further, increasing the voltage from 3 to 6 V increased the contact angle from 63.8° to 74.1°, indicating more hydrophobicity. However, rising voltage from 6 to 9 V caused an increase in the hydrophilicity properties.

ACKNOWLEDGEMENTS

The work was financially supported by Malayer University Research Grant No. 1400.

REFERENCES

1. Arsiwala, A., Desai, P., Patravale, V., "Recent advances in micro/nanoscale biomedical implants", *Journal of Controlled Release*, Vol. 189, (2014), 25-45. <https://doi.org/10.1016/j.jconrel.2014.06.021>
2. Bebell, L. M., Muiru, A. N., "Antibiotic Use and Emerging Resistance: how can resource-limited countries turn the tide?", *Global Heart*, Vol. 9, No. 3, (2014), 347-358. <https://doi.org/10.1016/j.gheart.2014.08.009>
3. Park, J., Lakes, R. S., *Biomaterials: An Introduction*, 3rd Ed., Springer Science & Business Media, (2007). <https://books.google.com/books/about/Biomaterials.html?id=bb6>

8wb0R_EAC

4. Elias, C. N., Lima, J. H. C., Valiev, R., Meyers, M. A., "Biomedical applications of titanium and its alloys", *Journal of the Minerals, Metals & Materials Society*, Vol. 60, No. 3, (2008), 46-49. <https://doi.org/10.1007/S11837-008-0031-1>
5. Gotman, I., Gutmanas, E. Y., "Titanium nitride-based coatings on implantable medical devices", *Advanced Biomaterials and Devices in Medicine*, Vol. 1, No. 1, (2014), 53-73. http://abiodem.com/download/files/abiodem_2014_no1_p53_gotman.pdf
6. Shanaghi, A., Mehrjou, B., Ahmadian, Z., Souri, A. R., Chu, P. K., "Enhanced corrosion resistance, antibacterial properties, and biocompatibility by hierarchical hydroxyapatite/ciprofloxacin-calcium phosphate coating on nitrided NiTi alloy", *Materials Science and Engineering: C*, Vol. 118, (2021), 111524. <https://doi.org/10.1016/j.msec.2020.111524>
7. Mehrjou, B., Dehghan-Baniani, D., Shi, M., Shanaghi, A., Wang, G., Liu, L., Qasim, A. M., Chu, P. K., "Nanopatterned silk-coated AZ31 magnesium alloy with enhanced antibacterial and corrosion properties", *Materials Science and Engineering: C*, Vol. 116, (2020), 111173. <https://doi.org/10.1016/j.msec.2020.111173>
8. Schultze, J. W., Lohrengel, M. M., "Stability, reactivity and breakdown of passive films. Problems of recent and future research", *Electrochimica Acta*, Vol. 45, No. 15-16, (2000), 2499-2513. [https://doi.org/10.1016/S0013-4686\(00\)00347-9](https://doi.org/10.1016/S0013-4686(00)00347-9)
9. Xiang, G. X., Li, S. Y., Song, H., Nan, Y. G., "Fabrication of modifier-free superhydrophobic surfaces with anti-icing and self-cleaning properties on Ti substrate by anodization method", *Microelectronic Engineering*, Vol. 233, (2020), 111430. <https://doi.org/10.1016/j.mee.2020.111430>
10. Kumar, G., Narayan, B., "Osseointegrated titanium implants: Requirements for ensuring a long-lasting, direct bone-to-implant anchorage in man", In Banaszkiwicz, P., Kader, D. (eds.), *Classic Papers in Orthopaedics*, London, Springer, (2014), 507-509. https://doi.org/10.1007/978-1-4471-5451-8_133
11. Masahashi, N., Mori, Y., Tanaka, H., Kogure, A., Inoue, H., Ohmura, K., Kodama, Y., Nishijima, M., Itoi, E., Hanada, S., "Bioactive TiNbSn alloy prepared by anodization in sulfuric acid electrolytes", *Materials Science and Engineering: C*, Vol. 98 (2019), 753-763. <https://doi.org/10.1016/j.msec.2019.01.033>
12. Beranek, R., Hildebrand, H., Schmuki, P., "Self-Organized Porous Titanium Oxide Prepared in H₂SO₄/HF Electrolytes", *Electrochemical and solid-state letters*, Vol. 6, No. 3, (2003), B12. <https://doi.org/10.1149/1.1545192>
13. Long, Y., Li, D. G., Chen, D. R., "Influence of Square Wave Anodization on the Electronic Properties and Structures of the Passive Films on Ti in Sulfuric Acid Solution", *Applied Surface Science*, Vol. 425, (2017), 83-94. <https://doi.org/10.1016/j.apsusc.2017.06.319>

14. Mohitfar, S. H., Mahdavi, S., Etminanfar, M., Khalil-Allafi, J., "Characteristics and tribological behavior of the hard anodized 6061-T6 Al alloy", *Journal of Alloys and Compounds*, Vol. 842, (2020), 155988. <https://doi.org/10.1016/j.jallcom.2020.155988>
15. Cheng, T. C., Chou, C. C., "The electrical and mechanical properties of porous anodic 6061-T6 aluminum alloy oxide film", *Journal of Nanomaterials*, Vol. 2015, (2015), 371405. <https://doi.org/10.1155/2015/371405>
16. Shih, T. S., Wei, P. S., Huang, Y. S., "Optical properties of anodic aluminum oxide films on Al1050 alloys", *Surface and Coatings Technology*, Vol. 202, No. 14, (2008), 3298-3305. <https://doi.org/10.1016/j.surfcoat.2007.12.002>
17. Masuda, H., Yada, K., Osaka, A., "Self-ordering of cell configuration of anodic porous alumina with large-size pores in phosphoric acid solution", *Japanese Journal of Applied Physics*, Vol. 37, No. 11A, (1998), L1340. <https://doi.org/10.1143/JJAP.37.L1340>
18. Zhang, J., Kielbasa, J. E., Carroll, D. L., "Controllable fabrication of porous alumina templates for nanostructures synthesis", *Materials Chemistry and Physics*, Vol. 122, No. 1, (2010), 295-300. <https://doi.org/10.1143/JJAP.37.L1340>
19. Wang, J., Wang, C. W., Li, Y., Liu, W. M., "Optical constants of anodic aluminum oxide films formed in oxalic acid solution", *Thin Solid Films*, Vol. 516, No. 21, (2008), 7689-7694. <https://doi.org/10.1016/j.tsf.2008.03.023>
20. Ghaforyan, H., Ebrahimzadeh, M., "Self-organized formation of hexagonal pore arrays in anodic alumina fabrication", *Journal of Materials Science and Engineering. B*, Vol. 1, No. 1B, (2011), 82-85. https://www.researchgate.net/profile/Hossein-Ghaforyan/publication/267773291_Self-Organized_Formation_of_Hexagonal_Pore_Arrays_in_Anodic_Alumina_Fabrication/links/56fa4b0508ae38d710a38580/Self-Organized-Formation-of-Hexagonal-Pore-Arrays-in-Anodic-Alumina-Fabrication.pdf
21. Chung, C. K., Liu, T. Y., Chang, W. T., "Effect of oxalic acid concentration on the formation of anodic aluminum oxide using pulse anodization at room temperature", *Microsystem Technologies*, Vol. 16, No. 8-9, (2010), 1451-1456. <https://doi.org/10.1007/s00542-009-0944-9>
22. Kumar, A., "Anodization of Titanium Alloy (Grade 5) to Obtain Nanoporous Surface Using Sulfuric Acid Electrolyte", *IETE Journal of Research*, Vol. 68, No. 5, (2020), 3855-3861. <https://doi.org/10.1080/03772063.2020.1780958>
23. Mehrjou, B.; Mo, S.; Dehghan-Baniani, D.; Wang, G.; Qasim, A. M., Chu, P. K., "Antibacterial and Cytocompatible Nanoengineered Silk-Based Materials for Orthopedic Implants and Tissue Engineering", *ACS Applied Materials & Interfaces*, Vol. 11, No. 35, (2019), 31605-31614. <https://doi.org/10.1021/acsami.9b09066>
24. Owens, D. K.; Wendt, R. C., "Estimation of the Surface Free Energy of Polymers", *Journal of Applied Polymer Science*, Vol. 13, No. 8, (1969), 1741-1747. <http://doi.org/10.1002/app.1969.070130815>
25. Zhou, X., Wu, F., Ouyang, C., "Electroless Ni-P alloys on nanoporous ATO surface of Ti substrate", *Journal of Materials Science*, Vol. 53, No. 4, (2018), 2812-2829. <https://doi.org/10.1007/s10853-017-1686-1>